
TAXONOMY-CONDITIONED HIERARCHICAL BAYESIAN TSB MODELS FOR HETEROGENEOUS INTERMITTENT DEMAND FORECASTING

A PREPRINT

Zong-Han Bai*

hu110048138@gapp.nthu.edu.tw

Po-Yen Chu*

b10704031@ntu.edu.tw

ABSTRACT

Intermittent demand forecasting poses unique challenges due to sparse observations, cold-start items, and obsolescence. Classical models such as Croston, SBA, and the Teunter–Syntetos–Babai (TSB) method provide simple heuristics but lack a principled generative foundation.

We introduce TSB-HB, a hierarchical Bayesian extension of TSB. Demand occurrence is modeled with a Beta–Binomial distribution, while nonzero demand sizes follow a Log-Normal distribution. Crucially, hierarchical priors enable partial pooling across items, stabilizing estimates for sparse or cold-start series while preserving heterogeneity. This framework provides a coherent generative reinterpretation of the classical TSB structure.

On the UCI Online Retail dataset, TSB-HB achieves the lowest RMSE and RMSSE among all baselines, while remaining competitive in MAE. On a 5,000-series M5 sample, it improves MAE and RMSE over classical intermittent baselines. Under the calibrated probabilistic configuration, TSB-HB yields competitive pinball loss and a favorable sharpness–calibration tradeoff among the parametric baselines reported in the main text.

1 Introduction

In operational settings, the value of a demand forecast lies not just in its numerical proximity to realized observations, but in its ability to support robust inventory decisions under extreme uncertainty Teunter et al. (2011).

Intermittent demand—long runs of zeros punctuated by occasional positives—poses a fundamental challenge to traditional forecasting because individual time series are often too sparse to provide reliable local evidence Croston (1972).

Planners in spare parts, long-tail retail, and hospital supplies face chronic issues with cold-start items and obsolescence, where miscalibrated forecasts propagate into systemic stockouts or excessive inventory (Syntetos and Boylan, 2005; Teunter et al., 2011). Two broad modeling routes dominate the literature. The first comprises exponential-smoothing (ES) decompositions, such as Croston’s method and its variants like the Teunter–Syntetos–Babai (TSB) approach Teunter et al. (2011). These heuristics remain attractive in industry due to their simplicity and scalability Yang et al. (2021); yet they lack a principled generative foundation, treat items in isolation (foregoing the benefits of information sharing), and are highly sensitive to smoothing constants Syntetos and Boylan (2005). The second route utilizes generative, distributional forecasting, often employing hierarchical Bayesian (HB) priors to partially pool information across a panel Pitkin et al. (2024).

This paper proposes **TSB-HB**, a minimalist generative bridge between these routes. We retain the operational intuition of TSB’s multiplicative structure—occurrence probability times positive size—but cast each factor into a coherent hierarchical generative core. We argue that for intermittent patterns, a **stable demand intensity** induced by hierarchical shrinkage is operationally preferable to chasing stochastic ripples in sparse local histories. By empirical-Bayes (EB) estimation, TSB-HB borrows strength from the full panel to stabilize sparse and cold-start series Robbins (1992). In this paper, *taxonomy-conditioned* means that Online Retail pooling groups are defined by ADI/CV^2 categories

*Equal contribution

(Smooth, Erratic, Intermittent, Lumpy) using thresholds 1.32 and 0.49 (Syntetos et al., 2005), while the M5 results use a single global pool. Groups are computed once from the in-sample window (ADI-CV² taxonomy); no time-varying regime switching is modeled. Our contributions are threefold.

First, we formulate a hierarchical, generative analogue of TSB that preserves its multiplicative decomposition while enabling principled panel-wise information sharing.

Second, we derive closed-form item-level posterior moments for occurrence and size, with low-dimensional EB hyperparameter fitting and $O(N)$ per-epoch forecasting suitable for large-scale retail catalogs.

Third, through fixed-origin experiments on Online Retail and M5 together with a walk-forward robustness check, we show that TSB-HB is a strong point-forecast baseline and delivers a favorable sharpness-calibration tradeoff in probabilistic forecasting.

The remainder of the paper is organized as follows: Section 2 reviews related work; Section 3 develops the TSB-HB model and its properties; Section 4 presents fixed-origin evaluations with protocol-robustness evidence; and Section 5 concludes. Additional ablations and extended diagnostics are provided in the supplement.

2 Related Work

Classical intermittent-demand forecasting began with Croston’s decomposition, which applies independent exponential smoothers to the inter-demand interval and the positive demand size, then forms a ratio to obtain a per-period mean forecast (Croston, 1972). Subsequent studies documented bias in the ratio estimator and proposed corrections such as the Syntetos–Boylan Approximation (SBA) and related variants that trade bias for variance under different assumptions. Overall accuracy in this family is highly sensitive to the choice of smoothing constants, and performance rankings can shift across error metrics and data regimes.

To better handle obsolescence, the Teunter–Syntetos–Babai (TSB) method smooths the period-by-period occurrence probability instead of interarrival times, ensuring updates on zeros and faster decay when demand ceases (Teunter et al., 2011). Follow-on refinements (e.g., mTSB) adjust the probability update while remaining within the ES heuristic paradigm and inheriting its dependence on smoothing hyperparameters (Yang et al., 2021). These approaches retain strong practical appeal due to their simplicity and interpretability but do not arise from a coherent generative model and do not share information across items.

An alternative line of work adopts generative, distributional models that explicitly account for zero inflation via hurdle or zero-inflated mechanisms, often coupled with hierarchical priors to enable partial pooling across a panel. Such models improve calibration, facilitate covariate inclusion, and stabilize estimates for sparse series, with recent applications to retail demand and related count processes (e.g., Pitkin et al., 2024). Deep learning methods extend this distributional perspective and can offer strong accuracy on large-scale datasets, though they may trade off interpretability and impose higher data or operational costs.

Intermittent-demand studies do not commit to a single law for positive sizes. In TSB’s numerical study, the logarithmic distribution was chosen for sizes because it is discrete, offers a tunable variance-to-mean ratio, and—combined with Poisson arrivals—yields negative-binomial totals; however, the authors explicitly note that other distributions such as Lognormal and Gamma could have been used (Teunter et al., 2011).

Taken together, prior work has not, to our knowledge, simultaneously provided (i) a coherent generative model that preserves the operational intuition of TSB’s multiplicative occurrence–size structure and (ii) panel-wise partial pooling with closed-form, scalable (e.g., EB) estimators suited to large catalogs. Approaches that achieve one of these aspects often either treat items in isolation or rely on heavier inference machinery, limiting scalability on intermittent retail panels.

3 Methodology

3.1 Setup, Notation, and Assumptions

We consider a panel of items $i \in \{1, \dots, N\}$ with item-specific horizons $t \in \{1, \dots, T_i\}$ and a fixed forecast origin $t_{0,i} \in \{1, \dots, T_i\}$. The in-sample (initialization) window is $\mathcal{T}_i^{\text{in}} = \{1, \dots, t_{0,i}\}$ and the evaluation window is $\mathcal{T}_i^{\text{oos}} = \{t_{0,i} + 1, \dots, T_i\}$. When a common origin is used, we write t_0 , \mathcal{T}^{in} , and \mathcal{T}^{oos} without item subscripts.

For each (i, t) we observe nonnegative demand $Y_{i,t} \geq 0$ and define the occurrence indicator $p_{i,t} = \mathbb{I}\{Y_{i,t} > 0\}$. When $p_{i,t} = 1$ a conditional positive-demand size is observed, denoted $s_{i,t} = Y_{i,t}$ and $\ell_{i,t} = \log s_{i,t}$; otherwise

$s_{i,t}$ is unobserved. Let $n_i = |\mathcal{T}_i^{\text{in}}|$ and $m_i = \sum_{t \in \mathcal{T}_i^{\text{in}}} p_{i,t}$. When $m_i > 0$, define $\bar{\ell}_i = \frac{1}{m_i} \sum_{t \in \mathcal{T}_i^{\text{in}}: p_{i,t}=1} \ell_{i,t}$ and $s_{\ell,i}^2 = \frac{1}{m_i-1} \sum_{t: p_{i,t}=1} (\ell_{i,t} - \bar{\ell}_i)^2$ (if $m_i > 1$).

Segment definition (ADI-CV² taxonomy, Online Retail). Segment assignment is computed only from $\mathcal{T}_i^{\text{in}}$. For each item with $m_i > 0$, we define

$$\text{ADI}_i = \frac{n_i}{m_i}, \quad \text{CV}_i^2 = \left(\frac{\text{sd}\{s_{i,t} : p_{i,t} = 1\}}{\text{mean}\{s_{i,t} : p_{i,t} = 1\}} \right)^2.$$

We then classify Smooth/Erratic/Intermittent/Lumpy using thresholds (1.32, 0.49) (Syntetos et al., 2005). Items with no positive observations in $\mathcal{T}_i^{\text{in}}$ are assigned to the global fallback pool.

Assumptions. (i) Our primary protocol is fixed-origin forecasting over $\mathcal{T}_i^{\text{OOS}}$; (ii) conditional on $p_{i,t} = 1$, positive sizes are Log-Normal on the original scale, with Gaussian log-size residuals; (iii) each item belongs to a pooling group $g(i) \in \{1, \dots, G\}$ and uses group-specific priors $\pi_i \sim \text{Beta}(\alpha_{g(i)}, \beta_{g(i)})$ and $\mu_i \sim \mathcal{N}(\mu_{0,g(i)}, \tau_{g(i)}^2)$; (iv) the initialization window estimates hyper-parameters and item-level posteriors; (v) no covariates are used in the main model.² In experiments, $g(i)$ uses ADI/CV² segments on Online Retail and a single global pool on M5.

3.2 TSB-HB: A Multiplicative Forecast with Hierarchical Shrinkage

The hierarchical dependencies and information-sharing mechanism are visualized in Figure 1.

Model (generative). For each item i in group $g(i)$:

$$\pi_i \sim \text{Beta}(\alpha_{g(i)}, \beta_{g(i)}), \quad \mu_i \sim \mathcal{N}(\mu_{0,g(i)}, \tau_{g(i)}^2).$$

For each period t :

$$p_{i,t} \mid \pi_i \sim \text{Bernoulli}(\pi_i),$$

$$\ell_{i,t} \mid (p_{i,t} = 1, \mu_i) \sim \mathcal{N}(\mu_i, \sigma_{g(i)}^2),$$

and

$$Y_{i,t} = \begin{cases} \exp(\ell_{i,t}), & p_{i,t} = 1, \\ 0, & p_{i,t} = 0. \end{cases}$$

This retains TSB's occurrence-times-size decomposition while introducing group-conditioned partial pooling.

Closed-form posteriors and point forecasts. For each item i , the point forecast remains multiplicative:

$$\hat{Y}_i = \hat{\pi}_i \cdot \hat{S}_i. \quad (1)$$

For occurrence, with $\mu_{\pi,g} = \alpha_g / (\alpha_g + \beta_g)$ and $\phi_g = \alpha_g + \beta_g$, the posterior mean is

$$\hat{\pi}_i = \frac{\alpha_g + m_i}{\alpha_g + \beta_g + n_i} = \lambda_{i,g} \cdot \frac{m_i}{n_i} + (1 - \lambda_{i,g}) \cdot \mu_{\pi,g}, \quad (2)$$

$$\lambda_{i,g} = \frac{n_i}{n_i + \phi_g} \in [0, 1].$$

Group hyperparameters are fit by empirical Bayes: (α_g, β_g) via Beta-Binomial marginal likelihood, and $(\mu_{0,g}, \tau_g^2, \sigma_g^2)$ via a random-effects marginal likelihood on item sufficient statistics $(m_i, \bar{\ell}_i, s_{\ell,i}^2)$; full objectives and optimizer details are in the supplement. For conditional positive sizes, posterior shrinkage on the log scale uses

$$k_i = \frac{\hat{\sigma}_{i,\text{proc}}^2}{\hat{\tau}_g^2}, \quad w_i = \frac{m_i}{m_i + k_i}, \quad (3)$$

$$\hat{\mu}_i = w_i \bar{\ell}_i + (1 - w_i) \hat{\mu}_{0,g}, \quad \hat{v}_{\mu,i} = \frac{\hat{\sigma}_{i,\text{proc}}^2}{m_i + k_i}. \quad (4)$$

²Extensions with covariates can be obtained by (a) a logistic link on π_i and (b) a linear mixed model on $\ell_{i,t}$; we focus on intercept-only pooling to isolate shrinkage.

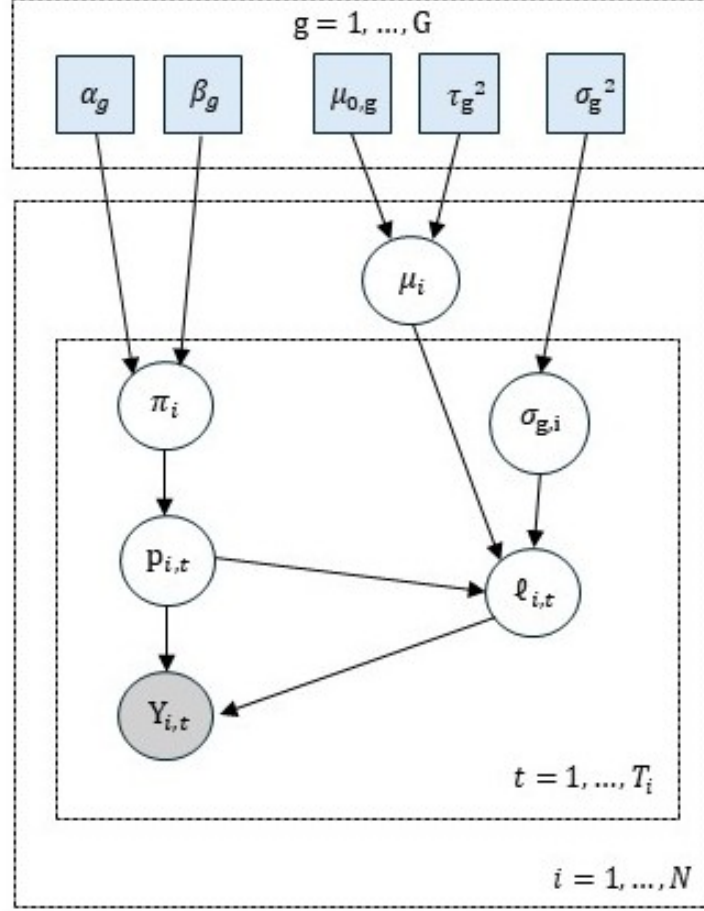


Figure 1: **TSB-HB graphical model (plate notation)**. The observed group index $g(i) \in \{1, \dots, G\}$ deterministically assigns group-specific hyperparameters $(\alpha_g, \beta_g, \mu_{0,g}, \tau_g^2, \sigma_g^2)$ to each item. Item-level latent variables (π_i, μ_i) generate the intermittent demand $Y_{i,t}$. Shaded nodes denote observed variables.

In the released configuration, $\hat{\sigma}_{i,\text{proc}}^2$ uses conjugate shrinkage toward the group scale with prior degrees of freedom $\nu = 20$ (supplement). The point-forecast size mean used in our implementation is

$$\hat{S}_i = \exp\left(\hat{\mu}_i + \frac{1}{2}\hat{\sigma}_{i,\text{proc}}^2\right). \quad (5)$$

This is a plug-in conditional mean that does not add posterior uncertainty of μ_i into the point estimate. Parameter uncertainty is incorporated only in probabilistic mode through (6). If $m_i = 0$, (3) gives $w_i = 0$ and $\hat{\mu}_i = \hat{\mu}_{0,g}$, yielding a coherent cold-start predictor. For probabilistic forecasts, we use the predictive log-variance

$$\hat{\sigma}_{i,\text{pred}}^2 = \hat{\sigma}_{i,\text{proc}}^2 + \hat{v}_{\mu,i}. \quad (6)$$

Relation to TSB. Equation (1) matches TSB’s multiplicative structure; the distinction is that (2) and (5) come from grouped EB posteriors rather than per-step EWMA. In TSB, smoothing parameters control temporal forgetting; here, credibility weights such as $\lambda_{i,g} = n_i/(n_i + \phi_g)$ and w_i control how strongly local evidence overrides pooled priors. This preserves interpretability while stabilizing sparse and cold-start series.

Probabilistic forecasting (optional). Beyond point means, TSB-HB yields a zero-inflated Log-Normal predictive law: mass $1 - \hat{\pi}_i$ at zero and a positive component with parameters $(\hat{\mu}_i, \hat{\sigma}_{i,\text{pred}}^2)$. For $q \in (0, 1)$, the predictive quantile

is

$$Q_i(q) = \begin{cases} 0, & \text{if } q \leq 1 - \hat{\pi}_i, \\ \exp\left(\hat{\mu}_i + \hat{\sigma}_{i,\text{pred}} \Phi^{-1}\left(\frac{q - (1 - \hat{\pi}_i)}{\hat{\pi}_i}\right)\right), & \text{if } q > 1 - \hat{\pi}_i. \end{cases}$$

The released probabilistic configuration adds (i) bootstrap averaging over $B = 20$ resamples of item sufficient-statistics rows and (ii) post-hoc location-scale calibration on quantiles (not on distribution parameters):

$$q^{\text{cal}} = (q_{0.5}^{\text{raw}} + \delta) + \lambda(q^{\text{raw}} - q_{0.5}^{\text{raw}}).$$

To avoid leakage, calibration uses only an internal chronological split of the initialization window (first 80% for fit, last 20% for calibration), and no out-of-sample targets are used in fitting or calibration. For fairness under nonnegative demand, all predictive quantiles from all methods are truncated below at 0 (and monotonized across quantile levels) before evaluation. The calibration objective and search grids are provided in the supplement.

3.3 Deterministic shrinkage properties

The posterior rules are convex shrinkage estimators. As sample size grows, item posteriors move monotonically from group priors toward item-level empirical statistics; in cold-start limits they revert to pooled priors. This behavior gives stable extrapolation for sparse series while preserving heterogeneity when local evidence is sufficient. A full derivation of monotonicity, bracketing, and the log-scale bias–variance tradeoff is provided in the supplement.

3.4 Large-sample behavior

Under standard regularity conditions for Beta–Binomial and random-effects EB blocks, group-level hyperparameter estimates are stable as panel size grows, and item-level posteriors increasingly reflect local evidence as n_i grows. We provide formal statements and assumptions in the supplement.

3.5 Computation and Complexity

Algorithm 1 TSB-HB Inference and Forecasting

```

1: procedure TSB_HB_INFERENCE(item sufficient statistics)
2:   for each group  $g$  do
3:      $(\hat{\alpha}_g, \hat{\beta}_g) \leftarrow \arg \max \prod_{i: g(i)=g} P(m_i | n_i, \alpha_g, \beta_g)$ 
4:      $(\hat{\mu}_{0,g}, \hat{\tau}_g^2, \hat{\sigma}_g^2) \leftarrow \text{EB\_RE}(\{\ell_{it} : g(i) = g\})$ 
5:   end for
6:   for each item  $i = 1$  to  $N$  do
7:      $g \leftarrow g(i)$ 
8:      $\hat{\pi}_i \leftarrow \frac{\hat{\alpha}_g + m_i}{\hat{\alpha}_g + \hat{\beta}_g + n_i}$ 
9:      $\hat{\sigma}_{i,\text{proc}}^2 \leftarrow \text{ConjugateVar}(\hat{\sigma}_g^2, s_{\ell,i}^2, m_i, \nu)$ 
10:     $k_i \leftarrow \hat{\sigma}_{i,\text{proc}}^2 / \hat{\tau}_g^2, \quad w_i \leftarrow m_i / (m_i + k_i)$ 
11:     $\hat{\mu}_i \leftarrow w_i \ell_i + (1 - w_i) \hat{\mu}_{0,g}$ 
12:     $\hat{v}_{\mu,i} \leftarrow \hat{\sigma}_{i,\text{proc}}^2 / (m_i + k_i)$ 
13:     $z_i \leftarrow \hat{\mu}_i + \frac{1}{2} \hat{\sigma}_{i,\text{proc}}^2$ 
14:     $\hat{S}_i \leftarrow \exp(z_i)$ 
15:     $\hat{Y}_i \leftarrow \hat{\pi}_i \cdot \hat{S}_i$ 
16:   end for
17:   return  $\{\hat{Y}_i\}_{i=1}^N$ 
18: end procedure

```

One pass over the initialization window computes sufficient statistics in $O(M)$ time ($M = \sum_i n_i$) and $O(N)$ memory. Group-wise Beta–Binomial fitting is a two-parameter optimization with per-iteration linear cost in the number of items per group. The size block estimates group random-effects hyperparameters and then applies item-wise conjugate variance updates in $O(N)$. Point prediction is $O(N)$ per epoch; probabilistic prediction is $O(NQ)$ for Q quantiles. Optional bootstrap uncertainty with B draws adds an $O(BN)$ term in probabilistic mode.

Variation (for ablation). A Gamma alternative for sizes (TSB-HB-Gamma) replaces the log-normal block by a conjugate Gamma–Gamma model: conditional on an item-specific rate $\beta_{s,i}$, positive sizes follow $S_{i,t} \mid \beta_{s,i} \sim \text{Gamma}(\alpha_s, \beta_{s,i})$, and the rates have a Gamma prior $\beta_{s,i} \sim \text{Gamma}(a, b)$. Empirical-Bayes estimates of (α_s, a, b) yield closed-form posterior means for item-level size, acting as shrinkage estimators between item means and panel priors. We report this sensitivity analysis in the supplement.

4 Experiments

We evaluate TSB-HB across point accuracy, probabilistic calibration, cross-dataset robustness, ablation analysis, and multi-horizon stability. Our experiments are designed to assess not only numerical accuracy but also distributional reliability and forecasting stability under sparse segments.

4.1 Experimental Setup

4.1.1 Dataset and Preprocessing

Primary evaluation is conducted on *Online Retail* (Chen, 2015). Preprocessing involves removing returns and zero-price transactions, capping quantities at the 99.5th percentile to mitigate outliers, and daily aggregation. Each SKU is densified with explicit zeros from its first to last transaction date, yielding 3,649 series. Additionally, we evaluate a seed-controlled sample of 5,000 series from the *M5* dataset (Howard et al., 2020) using the standard released pipeline. Detailed walk-forward evaluations are provided in the Appendix.

4.1.2 Evaluation Protocol

We adopt fixed-origin evaluation (Yang et al., 2021). For *Online Retail* (point and probabilistic), the first one-third of each series is used for initialization and the remaining two-thirds form the out-of-sample horizon. For the released *M5* point run, the fixed split uses initialization ratio 2/3 and evaluation ratio 1/3. In fixed-origin tables, every model is fit once on the initialization window and then forecasted over the full horizon without consuming out-of-sample targets for state updates. This defines a stable-horizon demand-intensity estimation task rather than short-horizon state tracking. For TSB-HB this implies one time-invariant point forecast per item across the out-of-sample horizon; for baselines with native multi-step trajectories (e.g., AutoARIMA and AutoTheta), we use their direct h -step forecasts from the same initialization fit and align each lead-time forecast to the corresponding out-of-sample timestamp. Walk-forward uses the same models but updates after each revealed block; detailed walk-forward rows are reported in the supplement. The probabilistic tables in the main text use the fixed protocol with full baseline mode and conformal baselines enabled. The TSB-HB probabilistic configuration follows the released setting: $\nu = 20$, bootstrap draws $B = 20$, location-scale calibration ratio 0.2, $\lambda \in [0.6, 1.2]$ with 13 grid points, and coverage-penalty weight 0.5 (seed 42). In probabilistic mode, calibration uses only the initialization window via an internal chronological split, while the out-of-sample horizon remains untouched until final evaluation.

4.1.3 Baseline Models

Point baselines in the main tables are Croston Classic, SBA, TSB, ADIDA, IMAPA, AutoARIMA, and AutoTheta (Nikolopoulos et al., 2011; Assimakopoulos and Nikolopoulos, 2000; Hyndman and Athanasopoulos, 2018; Garza et al., 2022; Kourentzes and Petropoulos, 2016). In our runs, TSB uses fixed $(\alpha_d, \alpha_p) = (0.5, 0.45)$, while ADIDA/IMAPA/AutoARIMA/AutoTheta follow StatsForecast defaults; when probabilistic intervals are requested from StatsForecast, AutoARIMA and AutoTheta use season length 7. Probabilistic comparisons in the main text combine parametric quantile models (TSB-HB, AutoARIMA, AutoTheta) with split-conformal residual-quantile calibration wrappers applied to point baselines (CP-CrostonClassic, CP-CrostonSBA, CP-ADIDA, CP-TSB, CP-IMAPA), using a chronological calibration ratio of 0.2 (Lei et al., 2018; Shafer and Vovk, 2007; Oliveira et al., 2024). We form $(1 - \alpha)$ intervals as $[\hat{y} + Q_{\alpha/2}(r), \hat{y} + Q_{1-\alpha/2}(r)]$ where $r = y - \hat{y}$ is the signed residual on the calibration split.

Reproducibility. All experiments in this paper are drawn from `tsb-hb/final_experiment_result` in the repository <https://anonymous.4open.science/r/tsb-hb-3843>.

4.1.4 Evaluation Metrics

Point evaluation uses MAE (Hyndman and Koehler, 2006), RMSE (Hyndman and Koehler, 2006), and RMSSE (Makridakis et al., 2022). MAE/RMSE are micro-averages over all evaluated (i, t) pairs:

$$\text{MAE} = \frac{1}{\sum_i |\mathcal{T}_i^{\text{oos}}|} \sum_i \sum_{t \in \mathcal{T}_i^{\text{oos}}} |y_{i,t} - \hat{y}_{i,t}|.$$

$$\text{RMSE} = \sqrt{\frac{1}{\sum_i |\mathcal{T}_i^{\text{oos}}|} \sum_i \sum_{t \in \mathcal{T}_i^{\text{oos}}} (y_{i,t} - \hat{y}_{i,t})^2}.$$

For RMSSE, let \mathcal{I} be the set of series with valid naive denominators, and define

$$D_i = \frac{1}{|\mathcal{T}_i^{\text{in}}| - 1} \sum_{t=2}^{|\mathcal{T}_i^{\text{in}}|} (y_{i,t} - y_{i,t-1})^2.$$

$$E_i = \frac{1}{|\mathcal{T}_i^{\text{oos}}|} \sum_{t \in \mathcal{T}_i^{\text{oos}}} (y_{i,t} - \hat{y}_{i,t})^2.$$

Our implementation computes

$$\text{RMSSE} = \sqrt{\frac{1}{|\mathcal{I}|} \sum_{i \in \mathcal{I}} \frac{E_i}{D_i}},$$

excluding series with $D_i \leq 0$ (constant or undefined scale) in accordance with the released code. For probabilistic evaluation, we report pinball loss at $q \in \{0.10, 0.25, 0.50, 0.75, 0.90\}$, mean pinball loss, empirical Coverage@80, and AIW@80 (Koenker and Bassett Jr, 1978; Gneiting and Raftery, 2007).

4.2 Point Forecasting on Online Retail

Table 1 summarizes the point forecasting performance on the *Online Retail* dataset. **TSB-HB** achieves the lowest RMSE (17.6930) and RMSSE (4.7875), representing a 5.5% reduction in RMSE relative to the standard TSB model. While the TSB baseline yields a slightly lower MAE, the substantial gains in squared and scaled error metrics indicate that the hierarchical Bayesian framework effectively mitigates large-scale forecasting errors, often caused by intermittent demand spikes, by shrinking individual series estimates toward informative group priors.

The results further suggest that **TSB-HB** provides a superior trade-off between accuracy and reliability. By pooling information across the panel, the model reduces error variance without significantly degrading absolute accuracy in quiet periods. Regarding computational efficiency, **TSB-HB** incurs a modest overhead (6.01 ms/SKU) compared to classical smoothing methods but remains significantly faster than statistical models like AutoARIMA (17.26 ms/SKU), demonstrating its viability for large-scale inventory replenishment systems.

Table 1: Point forecasting performance on Online Retail. **Bold** indicates the best performance, and underline indicates the second-best. Efficiency is measured as average inference time per SKU in milliseconds (ms).

Model	MAE	RMSE	RMSSE	Efficiency (ms)
CrostonClassic (1972)	6.3294	18.2320	5.1051	3.96
CrostonSBA (2005)	6.1953	18.1633	5.0692	3.77
AutoARIMA (2008)	6.5573	20.1451	4.8174	17.26
ADIDA (2011)	<u>5.6860</u>	<u>17.9617</u>	<u>4.7967</u>	4.03
TSB (2011)	5.5736	18.7272	4.8031	3.76
IMAPA (2016)	5.7000	17.9963	4.7970	3.85
AutoTheta (2012)	8.2862	22.4711	4.8550	4.65
TSB-HB (Ours)	5.7663	17.6930	4.7875	6.01

4.3 Segment-wise Performance Analysis

To analyze performance across demand patterns, we stratify series using the Average Demand Interval (ADI) and squared coefficient of variation (CV^2) (Syntetos and Boylan, 2005):

$$ADI = \frac{T}{N_p}, \quad CV^2 = \left(\frac{\sigma_p}{\mu_p} \right)^2$$

where N_p is the number of positive demand periods, and μ_p, σ_p are the mean and standard deviation of positive demand sizes. Series are categorized into four segments based on the thresholds $ADI = 1.32$ and $CV^2 = 0.49$.

Table 2 reports the RMSSE breakdown. **TSB-HB** shows marginal improvements in the *Intermittent* and *Lumpy* groups, where sparsity and variance make purely local estimation unstable. In *Smooth* and *Erratic* groups, the method remains competitive with classical baselines. Because several subgroup gaps are small and the Smooth/Erratic subsets are limited in size, we treat this table as directional evidence for taxonomy-conditioned pooling rather than a stand-alone significance claim.

Table 2: Segment-wise RMSSE breakdown based on ADI- CV^2 taxonomy. **Bold** indicates the best performance, and underline indicates the second-best.

Model	Interm. (1041)	Lumpy (2524)	Erratic (75)	Smooth (9)
CrostonClassic(1972)	8.9183	2.2006	<u>0.9301</u>	1.3819
CrostonSBA(2005)	8.8472	2.1990	0.9302	1.3782
AutoARIMA(2008)	8.3014	2.2556	1.0350	1.6679
ADIDA(2011)	8.2953	2.2021	0.9405	1.3935
TSB(2011)	8.2992	2.2151	1.0088	1.4088
IMAPA(2016)	8.2955	2.2026	0.9405	1.3935
AutoTheta(2012)	8.3271	2.3300	1.1765	1.5664
TSB-HB(Ours)	8.2849	2.1896	0.9272	<u>1.3849</u>

4.4 Probabilistic Performance and Distributional Quality

We evaluate distributional reliability using Pinball Loss and interval calibration. The Pinball Loss for a quantile q is defined as:

$$L_q(y, \hat{y}) = \max(q(y - \hat{y}), (1 - q)(\hat{y} - y))$$

where y and \hat{y} are the observed and predicted values. Table 3 shows that **TSB-HB** achieves the lowest Mean Pinball Loss (1.9192), substantially outperforming both parametric and conformal prediction (CP) baselines. Its superior performance at upper quantiles ($q75, q90$) demonstrates that the hierarchical Log-Normal prior accurately captures the long-tail behavior of demand spikes.

Table 3: Mean pinball loss across quantiles ($q \in \{0.1, \dots, 0.9\}$). **Bold** and underline indicate best and second-best performance.

Model	q10	q25	q50	q75	q90	Mean
CP-CrostonClassic	1.3585	2.2554	2.9033	3.0939	2.9951	2.5212
CP-CrostonSBA	1.3080	2.1866	2.8547	3.0911	3.0155	2.4912
AutoARIMA	0.6685	1.4704	2.9979	3.7263	<u>2.8390</u>	<u>2.3404</u>
CP-ADIDA	1.2551	2.1597	<u>2.7758</u>	<u>3.0327</u>	3.0233	2.4493
CP-TSB	1.1996	2.1010	2.7836	3.1806	3.2302	2.4990
CP-IMAPA	1.2768	2.1855	2.7891	3.0396	3.0278	2.4638
AutoTheta	<u>0.5204</u>	<u>1.4316</u>	3.2488	4.1637	3.0948	2.4919
TSB-HB(Ours)	0.4819	1.1894	2.2933	2.9731	2.6585	1.9192

Table 4 evaluates interval quality at the 80% nominal level. While CP methods produce narrower intervals (AIW ≈ 4.9), they suffer from under-coverage (0.7749). In contrast, **TSB-HB** provides a robust 0.8454 coverage. In retail context, this conservative coverage is preferable as it offers a safety buffer against unexpected spikes while maintaining sharpness during inactive periods, as visualized in Figure 2.

Table 4: Interval forecasting quality at 80% nominal level. **TSB-HB** achieves a superior balance between coverage and sharpness [cite: 242, 264].

Model	Coverage@80	CoverageGap	AIW@80	Relative Width
AutoARIMA	0.9144	0.1144	17.78	1.77x
AutoTheta	0.9409	0.1409	23.73	2.37x
CP-ADIDA	0.7749	0.0251	4.90	0.49x
TSB-HB (Ours)	0.8454	0.0454	10.03	1.00x

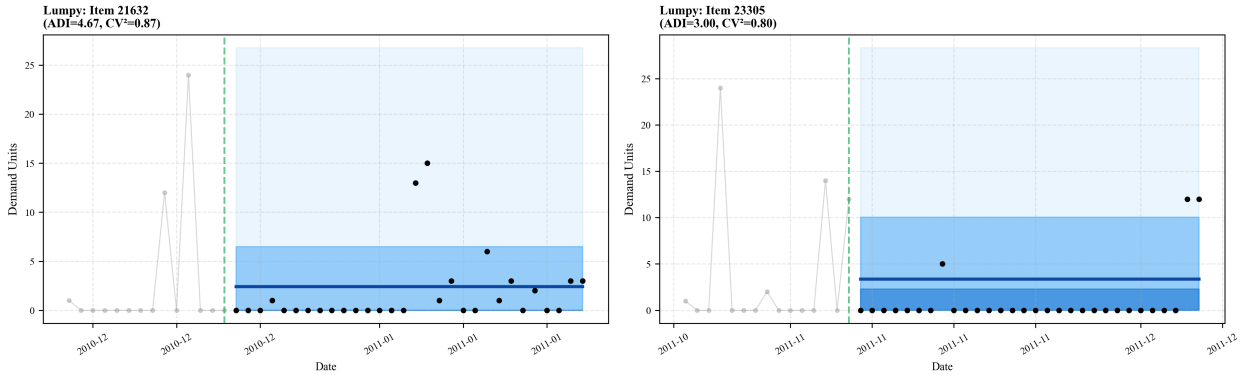


Figure 2: TSB-HB prediction intervals on two representative Online Retail SKUs. **Left: Intermittent segment** (high ADI, moderate CV^2): demand is mostly zero with occasional small positives. **Right: Lumpy segment** (high ADI, high CV^2): long zero stretches are punctuated by infrequent but large spikes. In both panels, black dots are observed demand, the dark blue line is the predictive median, and shaded regions denote the 80% prediction interval.

4.5 Robustness on the M5 Dataset

To assess the generalizability of our approach, we evaluate **TSB-HB** on 5,000 series sampled from the *M5* dataset (Howard et al., 2020). In the main *M5* table, TSB-HB uses a single global pooling group (no hierarchy grouping). Table 5 summarizes the point forecasting performance. **TSB-HB** achieves the lowest MAE (1.1771) and RMSE (2.8286), outperforming established baselines such as CrostonSBA and ADIDA. The consistency of these gains across distinct retail environments—moving from the *Online Retail* panel to the *M5* panel—suggests that the regularization benefit is not tied to a single dataset.

Table 5: Point forecasting performance on *M5*. **Bold** indicates the best performance, and underline indicates the second-best.

Model	MAE	RMSE	RMSSE
CrostonClassic (1972)	1.2345	2.9738	2.3539
CrostonSBA (2005)	<u>1.2076</u>	<u>2.8900</u>	2.3517
AutoARIMA (2008)	1.2289	3.0450	<u>2.3168</u>
ADIDA (2011)	1.2274	3.0669	2.3398
TSB (2011)	1.2672	3.2057	2.3612
IMAPA (2016)	1.2317	3.0916	2.3280
AutoTheta (2012)	1.2988	3.3220	2.3143
TSB-HB (Ours)	1.1771	2.8286	2.3759

Figure 3 shows reliability diagrams across quantile levels. While all models display mild over-coverage in sparse segments, TSB-HB remains closer to the diagonal, particularly at medium and high quantiles. This suggests that hierarchical shrinkage stabilizes predictive variance and improves distributional calibration without producing excessively wide intervals.

4.6 Ablation Study

We investigate the contributions of hierarchical shrinkage and distributional components on the *Online Retail* dataset.

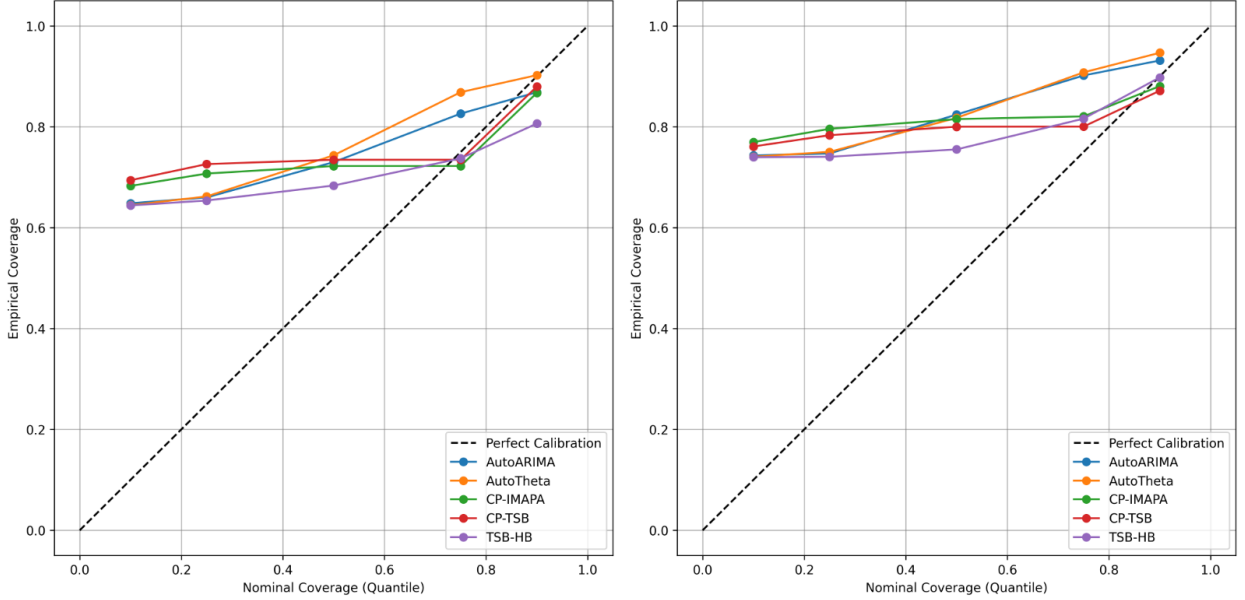


Figure 3: Calibration curves for Online Retail (Left) and M5 datasets (Right). TSB-HB exhibits consistent probabilistic calibration across different retail environments, with the predictive distributions closely following the ideal diagonal line.

4.6.1 Contribution to Point Forecasting

Table 6 summarizes performance across modeling strategies for occurrence (p) and size. While hierarchical shrinkage for occurrence ($\text{HB}(p)$) yields marginal gains over local estimation, pooling demand size ($\text{HB}(size)$) significantly reduces absolute and squared errors. The full model achieves the best performance, identifying size stabilization via hierarchical priors as the primary driver of point accuracy.

Table 6: Component ablation on point forecasting (Online Retail). **Bold** indicates the best performance.

Variant	MAE	RMSE	RMSSE
Local(p) + Local(size)	5.9931	17.7577	4.7912
HB(p) + Local(size)	5.9897	17.7519	4.7902
Local(p) + HB(size)	5.7753	17.7019	4.7892
Full HB (p + size)	5.7663	17.6930	4.7875

4.6.2 Contribution to Probabilistic Forecasting

We further evaluate process variance and calibration in Table 7. Omission of process variance substantially narrows intervals ($\text{AIW} \approx 5.1$) but triggers under-coverage and higher Pinball Loss, proving it essential for reliable predictive distributions. Calibration addresses mild over-dispersion, aligning empirical coverage with nominal targets while maintaining sharpness. In summary, hierarchical shrinkage stabilizes point forecasts, whereas variance and calibration ensure distributional reliability.

Table 7: Ablation on probabilistic forecasting (Online Retail). **Bold** indicates the best performance.

Variant	Mean Pinball	Coverage@80	AIW@80
Full HB	1.9193	0.8480	10.03
Full w/o process variance	2.0300	0.8067	5.09
Full w/o calibration	1.9158	0.9014	10.56
Ideal (Target)	-	0.8000	-

4.7 Mechanistic Evidence of Hierarchical Shrinkage

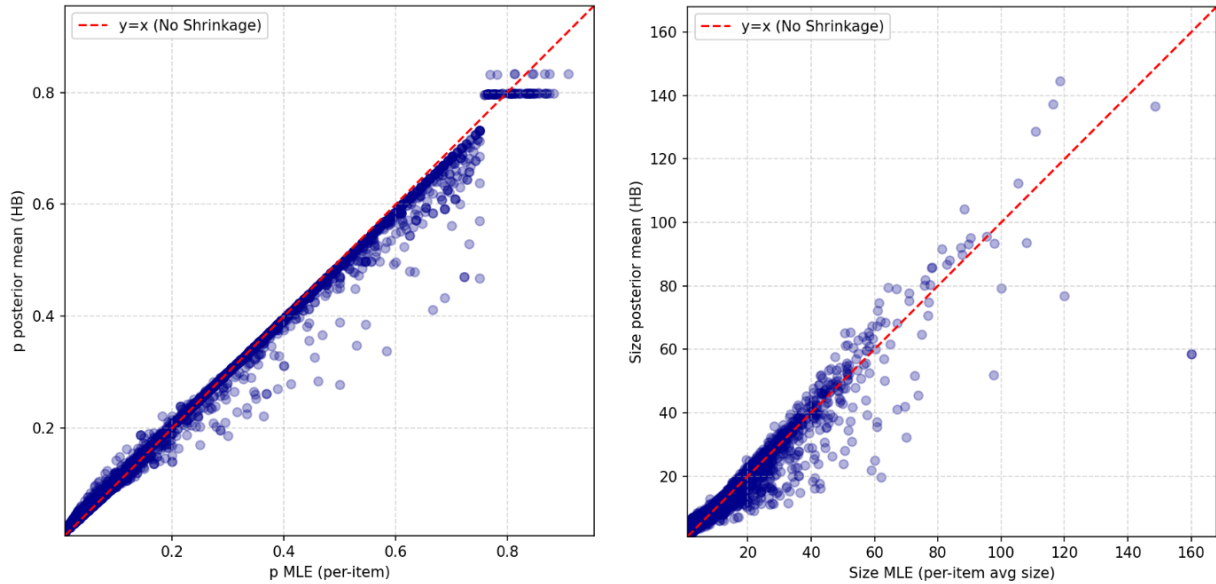


Figure 4: Visualization of hierarchical shrinkage for occurrence probability (left) and demand size (right). The posterior estimates (y-axis) are pulled toward the group mean relative to the MLE (x-axis), with the effect being most pronounced for low-volume series.

Figure 4 visualizes the adaptive regularization inherent in the hierarchical prior. By contrasting per-series Maximum Likelihood Estimates (MLE) against their posterior counterparts, we find that shrinkage is most pronounced for series with sparse observations or extreme, noisy MLE values. Conversely, well-supported series undergo minimal adjustment, as the model adaptively preserves local signals when data evidence is sufficient. This mechanism effectively stabilizes parameter estimation in the *Intermittent* and *Lumpy* regimes, where high individual variance is mitigated by borrowing strength from informative group-level priors.

4.8 Comparison with Deep Learning

We compare TSB-HB against RNN and DeepAR baselines under a prediction-only protocol at two representative forecast horizons, $h = 10$ and $h = 100$. These horizons respectively reflect short-term and long-term forecasting regimes, where error accumulation becomes increasingly critical under intermittent demand.

Across both horizons, **TSB-HB** consistently achieves the lowest RMSE and RMSSE (Table 8), indicating greater robustness against large forecast excursions. Although the RNN baseline attains lower MAE, its higher RMSE suggests increased sensitivity to large demand spikes—an issue particularly pronounced in sparse and bursty segments.

The efficiency gap is substantial. TSB-HB maintains sub-millisecond inference per series, whereas RNN inference time grows significantly with the forecast horizon, reaching 96.38 ms at $h = 100$. These results suggest that while neural models remain competitive in absolute deviation (MAE), our hierarchical Bayesian framework provides more stable scale-aware forecasts and superior scalability for large-scale industrial deployment.

5 Conclusion

This work proposed TSB-HB, a hierarchical Bayesian extension of the TSB paradigm that keeps the operational intuition of an occurrence–size factorization while supplying a coherent generative backbone. A Beta–Binomial layer regularizes demand occurrence and a pooled log-normal EB model stabilizes conditional sizes, yielding closed-form updates, scalable computation, and forecasts that interpretable occurrence–size decomposition.

Methodologically, TSB-HB (i) generalizes TSB into a coherent probabilistic model, (ii) introduces panel-wise partial pooling that is adaptive to data sparsity and cold starts, and (iii) supports distributional forecasts with optional in-sample calibration, without resorting to heavy inference machinery. Empirical studies indicate that the benefits

Table 8: Comparison with Deep Learning baselines on Online Retail at short ($h = 10$) and long ($h = 100$) forecast horizons. Efficiency reports total inference time (minutes) over the full test set.

h	Model	MAE	RMSE	RMSSE	Inference Time
10	TSB-HB (Ours)	4.6389	11.2842	0.8545	< 0.1 min
	RNN	3.2574	11.9384	0.8748	16 mins
	DeepAR	6.2449	17.2211	7.1509	4 mins
100	TSB-HB (Ours)	4.4946	11.7334	8.1704	< 0.1 min
	RNN	3.1318	12.5376	8.1971	17 mins
	DeepAR	7.2876	18.6228	9.9864	5 mins

concentrate where they matter operationally—intermittent and lumpy series—while maintaining the transparency valued in inventory settings.

The framework is intentionally minimalist. It does not yet model time-varying obsolescence or propagate hyperparameter uncertainty beyond plug-in EB. Future work may add state-space dynamics for both occurrence and size, integrate covariates and cross-item dependence, and target cost-aware policies aligned with service levels and capacity constraints.

References

- Vassilis Assimakopoulos and Konstantinos Nikolopoulos. The theta model: a decomposition approach to forecasting. *International journal of forecasting*, 16(4):521–530, 2000.
- Daqing Chen. Online Retail. UCI Machine Learning Repository, 2015. DOI: <https://doi.org/10.24432/C5BW33>.
- JD Croston. Forecasting and stock control for intermittent demands. *Journal of the Operational Research Society*, 23(3):289–303, 1972.
- Azul Garza, Max Mergenthaler Canseco, Cristian Challú, and Kin G. Olivares. StatsForecast: Lightning fast forecasting with statistical and econometric models. PyCon Salt Lake City, Utah, US 2022, 2022. URL <https://github.com/Nixtla/statsforecast>.
- Tilmann Gneiting and Adrian E Raftery. Strictly proper scoring rules, prediction, and estimation. *Journal of the American Statistical Association*, 102(477):359–378, 2007. doi: 10.1198/016214506000001437. URL <https://doi.org/10.1198/016214506000001437>.
- Addison Howard, inversion, Spyros Makridakis, and vangelis. M5 forecasting - accuracy. <https://kaggle.com/competitions/m5-forecasting-accuracy>, 2020. Kaggle.
- Rob J Hyndman and George Athanasopoulos. *Forecasting: principles and practice*. OTexts, 2018.
- Rob J. Hyndman and Anne B. Koehler. Another look at measures of forecast accuracy. *International Journal of Forecasting*, 22(4):679–688, 2006. doi: 10.1016/j.ijforecast.2006.03.001. URL <https://doi.org/10.1016/j.ijforecast.2006.03.001>.
- Roger Koenker and Gilbert Bassett Jr. Regression quantiles. *Econometrica: journal of the Econometric Society*, pages 33–50, 1978.
- Nikolaos Kourentzes and Fotios Petropoulos. Forecasting with multivariate temporal aggregation: The case of promotional modelling. *International Journal of Production Economics*, 181:145–153, 2016. ISSN 0925-5273. doi: <https://doi.org/10.1016/j.ijpe.2015.09.011>. URL <https://www.sciencedirect.com/science/article/pii/S0925527315003382>. SI: ISIR 2014.
- Jing Lei, Max G’Sell, Alessandro Rinaldo, Ryan J. Tibshirani, and Larry Wasserman. Distribution-free predictive inference for regression. *Journal of the American Statistical Association*, 113(523):1094–1111, 2018. doi: 10.1080/01621459.2017.1307116. URL <https://doi.org/10.1080/01621459.2017.1307116>.
- Spyros Makridakis, Evangelos Spiliotis, and Vassilios Assimakopoulos. M5 accuracy competition: Results, findings, and conclusions. *International Journal of Forecasting*, 38(4):1346–1364, 2022. ISSN 0169-2070. doi: <https://doi.org/10.1016/j.ijforecast.2021.11.013>. URL <https://www.sciencedirect.com/science/article/pii/S0169207021001874>. Special Issue: M5 competition.
- Konstantinos Nikolopoulos, Aris A Syntetos, John E Boylan, Fotios Petropoulos, and Vassilis Assimakopoulos. An aggregate–disaggregate intermittent demand approach (adida) to forecasting: an empirical proposition and analysis. *Journal of the Operational Research Society*, 62(3):544–554, 2011.

- Roberto I. Oliveira, Paulo Orenstein, Thiago Ramos, and João Vitor Romano. Split conformal prediction and non-exchangeable data. *Journal of Machine Learning Research*, 25(225):1–38, 2024. URL <http://jmlr.org/papers/v25/23-1553.html>.
- James Pitkin, Ioanna Manolopoulou, and Gordon Ross. Bayesian hierarchical modelling of sparse count processes in retail analytics. *The Annals of Applied Statistics*, 18(2):946–965, 2024.
- Herbert E Robbins. An empirical bayes approach to statistics. In *Breakthroughs in Statistics: Foundations and basic theory*, pages 388–394. Springer, 1992.
- Glenn Shafer and Vladimir Vovk. A tutorial on conformal prediction. *Journal of Machine Learning Research*, 9, 07 2007. doi: 10.1145/1390681.1390693.
- A. A. Syntetos and J. E. Boylan. The accuracy of intermittent demand estimates. *International Journal of Forecasting*, 21(2):303–314, 2005. doi: 10.1016/j.ijforecast.2004.09.009. URL <https://doi.org/10.1016/j.ijforecast.2004.09.009>.
- Aris A Syntetos, John E Boylan, and JD Croston. On the categorization of demand patterns. *Journal of the operational research society*, 56(5):495–503, 2005.
- Ruud H Teunter, Aris A Syntetos, and M Zied Babai. Intermittent demand: Linking forecasting to inventory obsolescence. *European Journal of Operational Research*, 214(3):606–615, 2011.
- Youpeng Yang, Chenyi Ding, Sanghyuk Lee, Limin Yu, and Fei Ma. A modified teunter-syntetos-babai method for intermittent demand forecasting. *Journal of Management Science and Engineering*, 6(1):53–63, 2021.